

# Radiation damage in the Chandra X-ray CCDs

G. Prigozhin, S. Kissel, M. Bautz, C. Grant, B. LaMarr, R. Foster, G. Ricker, G. Garmire

Center for Space Research,  
Massachusetts Institute of Technology,  
Cambridge, Massachusetts 02139

## ABSTRACT

Front side illuminated CCDs comprising focal plane of Chandra X-ray telescope have suffered some radiation damage in the beginning of the mission. Measurements of CTI and dark current at different temperatures led us to conclusion that the type of damage is inconsistent with the much studied type of damage created by protons with energies higher than 10 MeV. Intensive ground based investigation showed that irradiation of CCD with low energy protons (about 100 keV) results in the device characteristics very similar to the ones of the flight chips (very low dark current, the shape of the CTI temperature dependence). We were able to reliably determine that only image section of the flight chips was damaged and therefore only fast transfer from image to frame store section was affected. We have developed several techniques in order to determine the parameters of the electron traps introduced into the transfer channel of the irradiated device. One of them is based on the analysis of the amplitude of the signal in the pixels trailing the pixel that absorbed an X-ray photon of known energy. Averaging over large number of photons allowed us to get high signal/noise ratio even for pixels with extremely low signal far behind the X-ray event. Performing this analysis at different temperatures we were able to measure trap density, emission time constant, and trap cross section. Another technique is based on the analysis of the tail behind the events of very high amplitude, such as cosmic ray hits.

At least 3 different types of traps were detected, two of them with short time constants in the range from tens to a few hundred microseconds. The most damaging for the device performance is the third one with longer time constant in the millisecond range.

The measurement of the trap parameters allows us to accurately model charge transfer inefficiency and helps to choose optimal operational parameters, and eventually will lead to techniques that may noticeably improve performance of a damaged CCD.

**Keywords:** Charge Coupled Devices, X-ray spectroscopy, radiation damage, electron traps

## 1. INTRODUCTION

Soon after Chandra X-ray Observatory was launched into orbit and produced first images of the superb quality, the CCD focal plane was moved out of the focus of the telescope into the position where it could see the calibration source. An analysis of the calibration source data immediately revealed that all of the CCD chips had suffered some damage causing a significant jump in the charge transfer inefficiency (CTI). This triggered the most intensive investigation both of the type of the damage and the reasons that caused it. Originally high energy protons were considered the biggest threat to the Observatory due to their penetrating and damaging properties and also due to their high density in the space environment. Because of that intensive studies were conducted of the CCD damage by protons in the tens of MeV range.<sup>2-5</sup> It became clear very soon, though, that the type of the damage the Chandra devices had experienced is inconsistent with the results obtained in our lab by irradiating the Chandra-like CCDs with 40 MeV and 10 MeV protons. The main difference was extremely low dark current of the flight devices, even when the focal plane temperature was elevated to -50 C. Devices irradiated on the ground showed several orders of magnitude higher dark current at the same temperature. Also, the dependence of the CTI on temperature looked different for the ground irradiated chips.

We started to look for another type of damaging irradiation which could produce flight-like results. There seem to be no data in the literature on the damage caused by low energy protons (100 – 200 keV) and we implemented

---

Further author information: (Send correspondence to G.P.)  
G.P.: E-mail: gyp@space.mit.edu

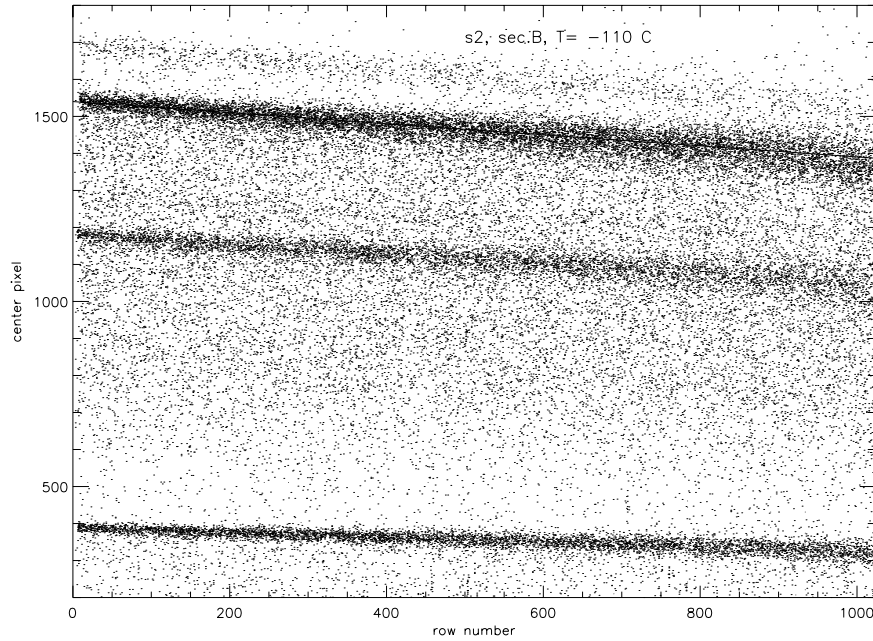


**Figure 1.** Pulseheight of the center pixel as a function of row number at -110 C for the damaged flight device S2.

a series of experiments irradiating CCDs with low energy protons. The most credible explanation now seems to be that the damage was caused by the low energy protons leaking through the telescope mirror during the radiation belt passages. The detailed discussion of the Chandra radiation environment and the details of the mechanism of the proton penetration through the telescope structure will be published elsewhere.<sup>1</sup> In this paper in the sections 2,3 we focus on the mechanism of the damage in the CCDs and the techniques we have developed to measure electron trap parameters. Another half of the paper (the section 4) describes our low energy proton experiment and related results, which we hope can lead to significant improvement of flight instrument performance.

## 2. CHARACTERIZATION OF THE DAMAGE IN THE FLIGHT DEVICES

One of the most meaningful ways to demonstrate the transfer inefficiency in a CCD is to plot the pulseheight of the X-ray event as a function of row number when the CCD is illuminated with the monochromatic source of X-rays. A typical example of such a plot for the damaged flight device S2 looking at the calibration source is shown in Fig. 1. The focal plane temperature during this measurement was maintained at  $-110^0$  C. Each dot in this plot represents an amplitude of the center pixel of an X-ray event, pixels adjacent to the center being ignored. Three emission lines can be clearly seen in the source spectrum as areas with the high density of the dots:  $Al K$ ,  $Ti K$  and  $Mn K_{\alpha}$ . Much weaker  $Mn K_{\beta}$  can also be observed near the top of the plot. The amplitude of the pulseheight for each of the emission lines gets smaller at the higher row numbers as charge packets lose charge in every transfer from pixel to pixel. In the beginning of the mission each emission line on this plot was absolutely flat, the width of each line also stayed the same across the entire device.

Extremely important feature of this plot is that the pulseheight-vs-row dependence is linear near the bottom of the image section and does not have a roll off or flattening at small row numbers. This is a strong indicator that unlike the image section of the device the frame store section was not damaged. When the frame store is irradiated and electron traps are introduced into its transfer channel, charge packets formed near the bottom of the image section will travel through the empty traps in the frame store section and experience much heavier charge losses than the following packets which go over the pixels with partially filled traps. As a result pulseheight-vs-row dependence typically curves down at the bottom of the image section in the frame transfer CCDs with both sections irradiated.

Another fact that helped to establish reliably that frame store section was not damaged is that the pulseheight amplitude near the bottom of the image section is the same as it was in the beginning of the flight before the charge transfer quality deteriorated. If the frame store section were damaged, the signal would lose some fraction of charge

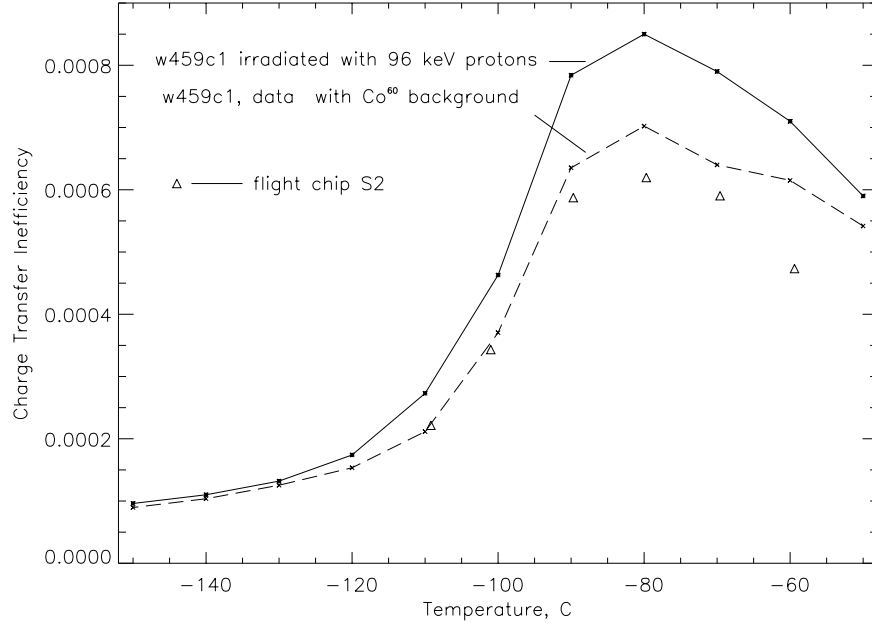


**Figure 2.** Temperature dependence of CTI for the damaged flight device S2 and device w459c1 irradiated by 102 keV protons.

passing through the damaged section and the amplitude of the signal from bottom rows inevitably would become lower.

The undamaged state of the frame store section and of the serial register became an important clue in the search of the damage mechanism. ACIS focal plane was constructed in such a way that the frame store section of each chip and the serial registers with the output nodes are protected by a gold plated aluminum shield. The shield has varying thickness, with the minimum being 2.54 mm thick. This explains why only image section of the CCD suffered some radiation damage, but it also implies that the spectrum of the damaging irradiation was very soft. It immediately ruled out protons in the tens of MeV range as the source of radiation damage because they would easily penetrate the thin aluminum shield.

Another strong argument in favor of low energy protons is that only frontside illuminated devices in the ACIS focal plane lost transfer efficiency. Two backside illuminated chips did not change. This means that the 40 microns thick substrate of the backside illuminated device was able to stop the flux of the damaging particles from hitting the transfer channel of the device on the unexposed surface of the wafer, and sets even stricter limit to the upper value of the radiation particle's energy. Calculations showed that the proton energy have to be lower than 2 MeV in order to be shielded by the substrate. There is also low energy limit to the particle's energy because the protons have to penetrate the optical blocking filter and the polysilicon gates of the frontside illuminated device to reach the buried channel. This requires the proton energy to be somewhat higher than 50–75 keV.

In our attempt to reproduce the characteristics of the flight devices we tried to irradiate the CCDs with electrons, but could not produce enough bulk damage for the CTI values to be consistent with the flight chip results.

Irradiation of the CCD with 102 keV protons brought the desired effect. Device w459c1, manufactured in the same lot with ACIS flight devices, was irradiated at Goddard Space Flight Center Van De Graaf generator. The dark current stayed very low, two orders of magnitude lower than for the devices irradiated with 40 MeV protons. And most importantly, the temperature dependence of the CTI which reflects a unique blend of electron traps in the transfer channel of the device looks very similar for the flight device and the ground irradiated one. CTI as function of temperature for the flight chip S2 and for the chip w459c1 is plotted on the Fig. 2. The qualitative agreement between flight and ground based data is good, some discrepancy seen in the Figure 2 can be explained by several factors. One of them is that the dose of proton flux in the ground experiment was based on the estimates of the flight dose and, of course, it is not possible to guess exactly the right number. Besides that, the flight chip sees significant level of background irradiation, and it is very difficult to reproduce similar environment on the ground.

We made an attempt to simulate cosmic background by placing a strong  $Co^{60}$  source close to the CCD during the measurement process. It obviously has a strong effect (see Fig. 2), moving a CTI curve much closer to the flight device data points. But still, the spectrum of the  $Co^{60}$  source is very different from the space radiation environment.

To investigate further the details of the damage mechanism we implemented the techniques described below.

### 3. PARAMETERS OF ELECTRON TRAP IN THE CHANNEL OF THE FLIGHT CCDS

The temperature dependence of CTI can provide an information about the energy trap parameters. The most common technique was described in,<sup>6,4</sup> but it does not allow to decouple the trap energy level and the trap cross section, thus making trap identification somewhat ambiguous. Besides that, the technique is based on the implicit assumption that the distance between all the X-ray events is always the same, which in reality is not true.

We have developed a new technique of measuring trap parameters which is in essence analogous to the DLTS (Deep Level Transient Spectroscopy) – a common way of trap characterization in semiconductor technology. Like in DLTS the traps are filled first and then the detrapping process is observed. Doing that at different temperatures allows to determine both trap energy level and its emission cross section. A valuable feature of our technique is that unlike the general DLTS, the location of the sampled traps is restricted to precisely the location of the signal charge in the buried channel, which is an extremely narrow region. Besides that, our technique is much more sensitive and can detect low concentration of traps due to the ability of CCD to detect miniscule amounts of charge transferred over long distances in the bulk of silicon. Our technique of watching the trailing pixels has something in common with EPER technique described long time ago by Janesick,<sup>7</sup> but is implemented in an entirely different way.

Irradiation of the CCD with protons introduces defects into the transfer channel of the device and these defects act as the electron trapping sites. When signal charge arrives to a pixel potential well the traps inside the volume occupied by electrons will become populated. The usual assumption is that capture time is small compared to pixel storage time and all the traps inside the volume of signal charge get filled. This assumption is very important when calculating the density of traps in the channel, it has no effect though on determining time constants of the trap, which is our major focus at this point. After the charge is transferred into the next pixel the traps start to emit the electrons back into the empty potential well. The same process is repeated for each of the following pixels behind the X-ray event, the integration time for collecting of the reemitted charge is the same for each of the trailing pixels. Thus a tail is formed behind the pixel containing the signal charge. According to the Shockley-Read-Hall theory the detrapping process decays exponentially with time with emission time constant  $\tau_e$  being determined by the the following formula:

$$\tau_e = \frac{\exp(E_t/kT)}{\sigma_t v_{th} N_c}$$

where  $E_t$  is energy level of the trap below the conduction band,  $\sigma_t$  is the trapping cross section,  $v_{th}$  - thermal velocity of electrons and  $N_c$  - effective density of states in the conduction band.

#### 3.1. Tails behind X-ray events

If one looks into the raw frames downloaded from the observatory, there can be clearly seen tails several pixels long behind the X-ray events formed near the top of the frame. The shape of the tail can tell the emission time constant of the trap. Deciphering the time constant may become a tricky business due to the possibility of having several different types of traps with different time constants. Another complication is that signal in the tail behind each individual event is small (especially several pixels behind the event), just a few ADUs, being comparable or smaller than the readout noise of the device. We solved this problem using the power of statistical approach. The trailing pixel amplitude was averaged over big number of the monochromatic X-ray events originating in the same region of the CCD (and hence undergoing the same number of transfers). The sample histograms of the signal in the trailing pixels are shown in Fig. 3. Histograms of a few trailing pixels are shown, the centers of the histograms shift down for the pixels that are further away. Also shown is a histogram of the pixel in front of the center, and as expected, it is centered around zero. Each of the histograms is then fitted with a gaussian and the centroids of the gaussians are plotted as a function of time behind the central pixel of the event forming the reemitted charge profile. Examples of the trailing pixel amplitudes at three different focal plane temperatures are shown in Fig. 4. The amplitudes of the trailing pixels seem to follow an exponential function very well, the quality of the fit improves dramatically though when two exponentials with different time constants are used. This is a clear indication that there are several types of traps present in the channel of the device. This is not surprising, since experiments described by other workers<sup>4,5</sup>

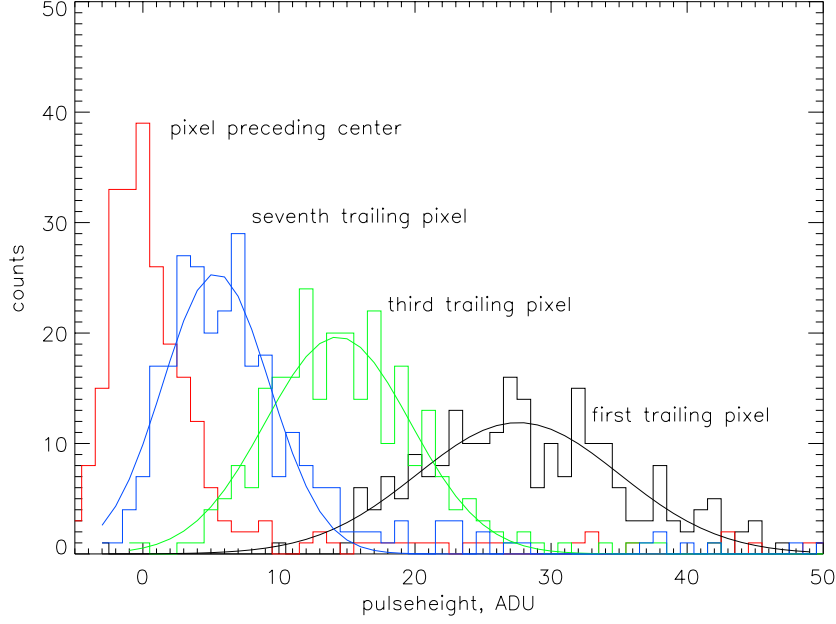


**Figure 3.** Histograms of the pulseheights in the trailing pixels behind the center of the event. All  $Mn K_{\alpha}$  events were selected from the rows above 700. Focal plane temperature -110 C.

at higher proton energies indicate multiple energy levels present. Besides that, an attempt to fit the data points with a single exponential function implied that the charge reemitted back into the trailing pixels is approximately two times smaller than the charge lost by the center pixel. The loss can be easily determined from the pulseheight-vs-row dependencies. The only explanation could be that there exists another trap with a long time constant, so that the charge reemitted by this trap is spread over large number of trailing pixels and its contribution into any particular pixel is very small.

The results of the two-exponential fit (solid lines in Fig. 4) suggest that in addition to the time constant of the order of  $100 \mu s$  (corresponding values are printed on each plot) there is another trap with time constant in the  $ms$  range. We do not show the values for this trap because they cannot be very accurate - making fit to the first 20–30 trailing pixels it is possible to measure only short time constants that have comparable time scale. The longer time constants require a different approach. Still, the densities of both traps could be measured, each of them contribute about 40% to the total charge loss.

The noticeably higher amplitude of the very first trailing pixel in the plot for  $T = -115^{\circ} C$  indicates that at low temperatures we start seeing the third trap with yet shorter time constant, which did not come into play at warmer temperatures. But again, the time constant for this trap cannot be accurate, the trailing charge from this trap can be clearly seen only in the very first trailing pixel which is not enough to make a meaningful exponential fit. The density of this trap is small – it accounts for only about 1.5% of the lost charge.

The measurements of the tail indicate that about 20% of the loss is unaccounted for. This means that there must be some other trap with longer time constant which could not be detected by this technique. This fact is consistent with the results described below in the section about “squeeze” technique.

### 3.2. Tails behind cosmic ray events

The CCDs in the Chandra focal plane experience numerous hits by high energy cosmic particles. Some of them produce signal of a very high amplitude, often saturating the readout circuits. The corresponding amplitude in the trailing pixels after such an event is also very high. These events present another opportunity to measure the time constants of the trap reemission process. Unlike the X-ray events, the amplitude of the signal in the cosmic ray tail stays above noise level for a long time, making it possible to measure long time constant for a single event. In this case it does not make sense to average pixel amplitudes of different traces because the center pixel amplitude is always different for cosmic ray events – they are not monochromatic. Instead, the time constants measured separately for

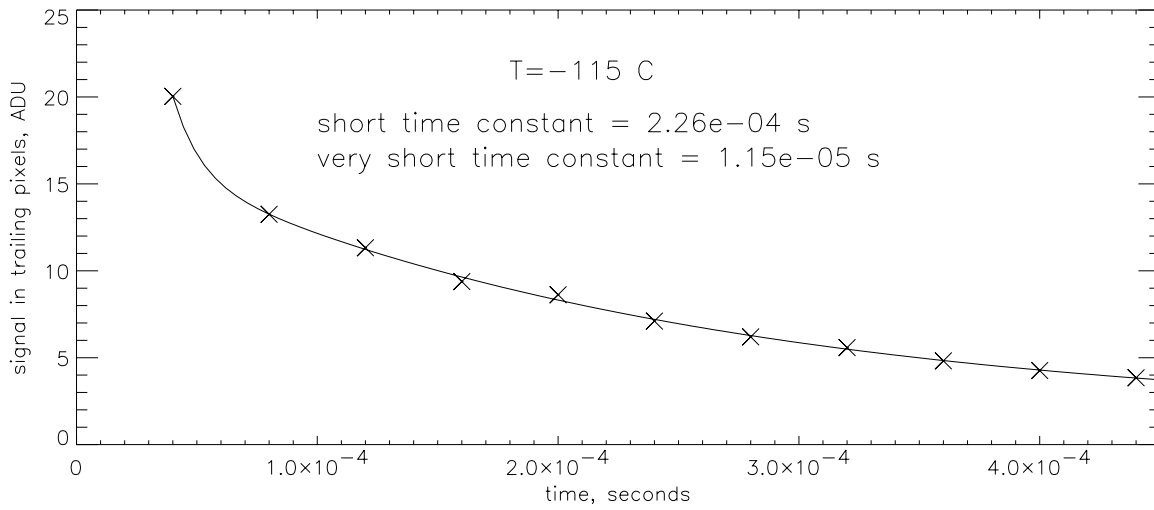
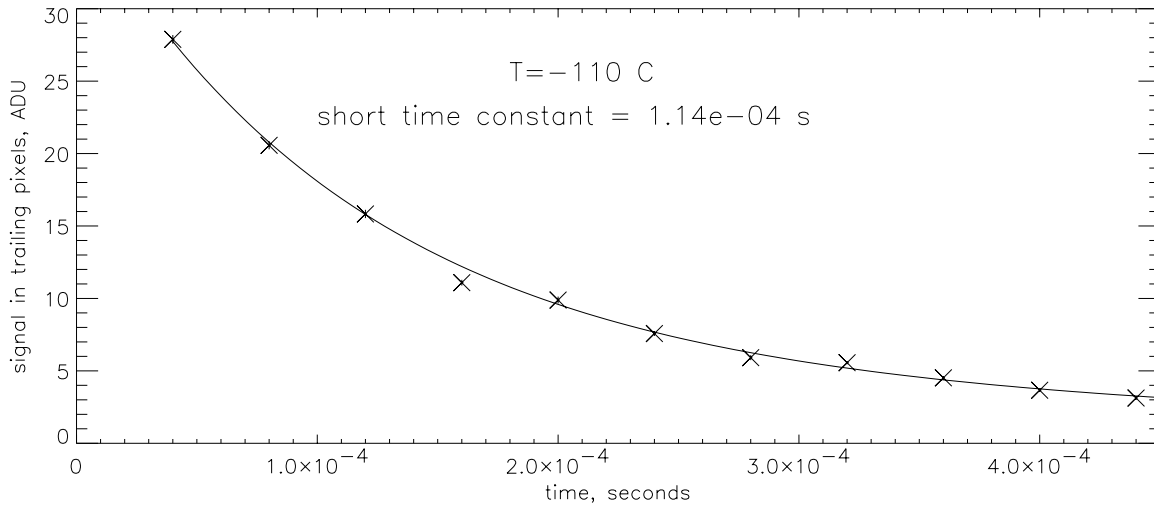
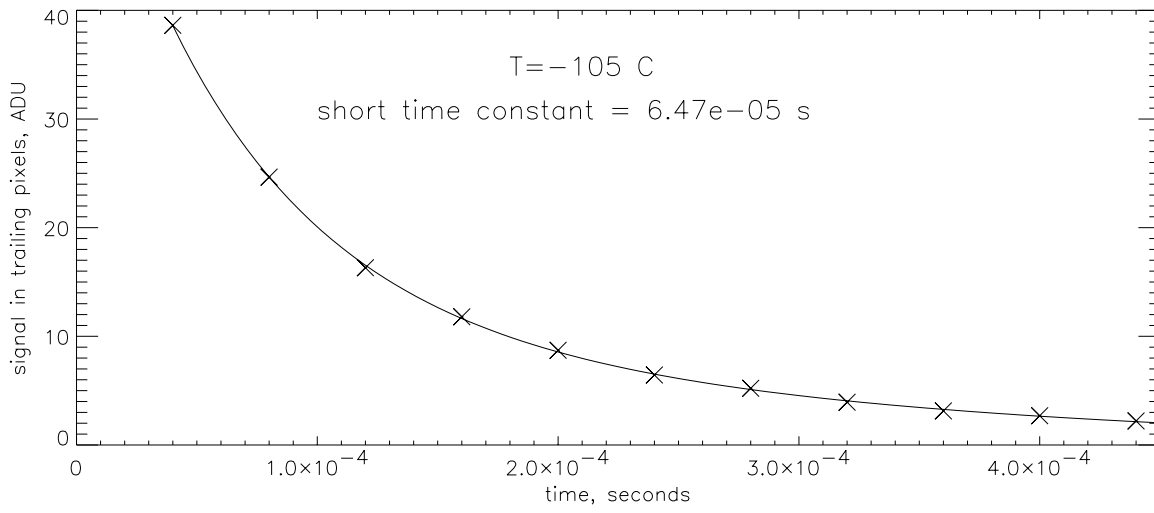


**Figure 4.** Amplitude of the signal in the trailing pixels as a function of time at focal plane temperatures -105, -110, and -115 C.

each of the appropriate tails were averaged. For the data sets at each temperature we were able to find An example of the trailing pixel amplitudes and a multiexponential fit to it is shown in Fig. 5. The fit is not ideal, but results

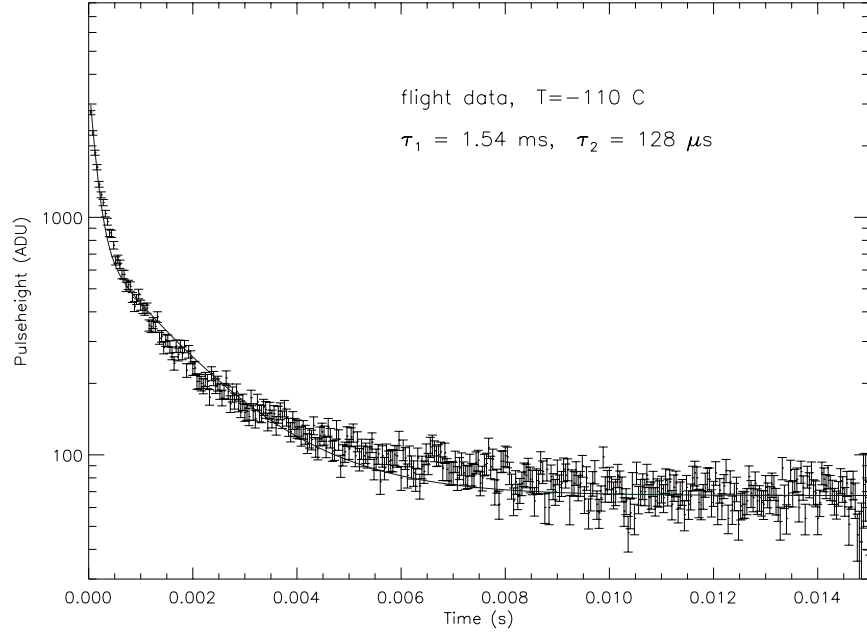


**Figure 5.** Amplitudes of the trailing pixels behind a cosmic ray hit of significant amplitude.

are pretty robust. Making a multiexponential fit we used the short time constant determined in section 3.1 as a fixed parameter.

At each temperature a fit was made to all available cosmic ray events which had appropriate amplitude and location. The time constants were averaged over all the cosmic rays at a given temperature. The results are shown in the next section on the Fig. 6

### 3.3. Trap identification

In order to determine the trap energy and the cross section the emission time constants extracted by the techniques described in the previous two sections are presented in the Arrhenius type plot of  $\ln(\tau_e T^2)$  as a function of  $1/T$  (Fig. 6). According to the theory it should be a linear function, since

$$\ln(\tau_e T^2) = \frac{E_t}{kT} - \ln(A\sigma)$$

where material parameter  $A = 1.6 \times 10^{21} \text{ cm}^{-2}$ .

It is widely accepted that divacancy is one of the defects introduced into silicon during neutron and proton irradiation. Divacancy is formed when two vacancies generated by irradiation are combined together in a stable immobile complex. The energy level of one of the electron traps associated with it is in the range of 0.2-0.23 eV, according to different sources. The solid line on Fig. 6 represents published divacancy trap parameters ( $E_t = 0.21 \text{ eV}$ ,  $\sigma_t = 6 \times 10^{-16} \text{ cm}^2$ ) to show that they are close to our experimental results.

Two rectangular points on the Fig. 6 represent the shortest time trap detected at the lowest temperatures ( $-114.7^\circ$  and  $-118.7^\circ \text{ C}$ ) of the focal plane. The dotted line shows a behavior of the trap with energy  $E = 0.16 \text{ eV}$  and cross section  $\sigma = 2.1 \times 10^{16} \text{ cm}^2$ , parameters that are close to published values for the so called O-V (oxygen-vacancy) trap. This trap is likely to be found in the buried layer of the CCD because near surface layer of the device must be rich in oxygen introduced during the surface oxidation.

We were not able to associate the third trap with slower time constants with any published trap parameters. Our measurements for this trap are the least reliable and this will require further work.

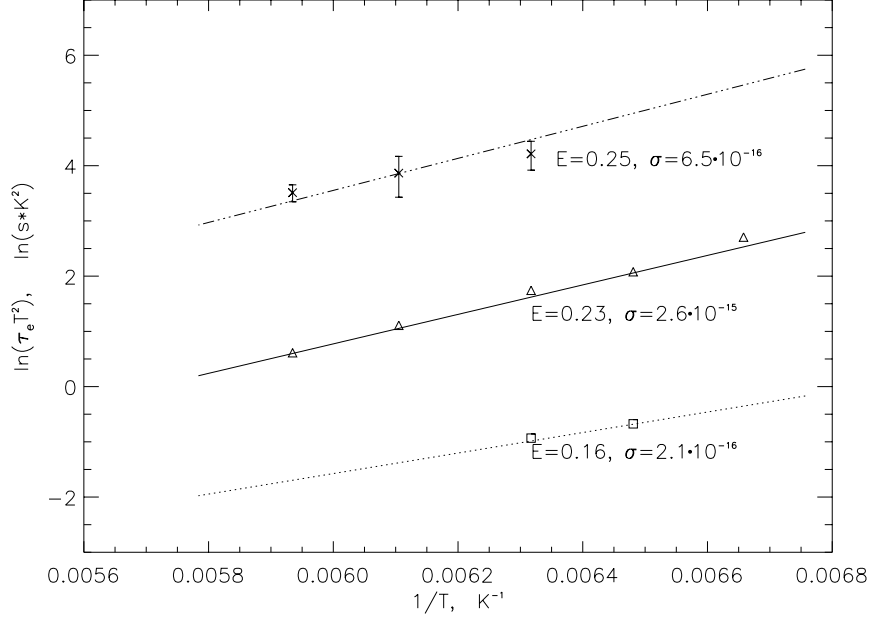


**Figure 6.** Arrhenius plot of the emission time as a function of temperature.

The most damaging for the device performance is this trap with long time constant in the millisecond range. For this trap the emission time is comparable to the time between events in the same column. As a result the loss of charge in a signal packet depends on the distance to the previous event and this leads to significant loss of the energy resolution near the top of the image section, because the distance between events can vary a lot. This trend is quite obvious in Fig. 1 where the width of each line is noticeably bigger at the end of the frame.

The traps with shorth time constants also cause the charge loss, but this loss depends only on the number of transfers (in other words, row number). The loss is not a function of prehistory, all the traps are empty when the next charge packet arrives. For such traps it is possible to implement a relatively simple correction algorithm in the processing software and significantly improve the device performance. For the long time constant traps correction is a much more difficult problem because all the previous events have to be taken into account. But still, such a correction can be done if the trap densities and time constants are known. This was a one of the strongest motivations behind the trap parameters measurement.

#### 4. GROUND BASED EXPERIMENT

As we mentioned above, the device w459c1 was irradiated with 102 keV protons at Van De Graaf accelerator. The total dose recieved by the device was  $3.6 \times 10^7$  protons/cm<sup>2</sup>. The dose was chosen at this level following our estimates of the dose recieved by the flight devices. The CCD was irradiated at room temperature. The device was subjected to intensive testing in order to establish whether the type of the damage is similar to that of the flight device. The nearly identical shape of the temperature dependence of the CTI suggests that the defect composition in both flight and ground irradiated devices is similar. To confirm that we conducted emission time constants measurements using the trailing pixel technique described in section 3.1.

##### 4.1. X-ray tails

We implemented the same X-ray trailing pixel technique as described in 3.1. The device was illuminated with  $Fe^{55}$  source and the trailing pixels behind  $Mn K_{\alpha}$  events were analyzed. The chip was at the same time illuminated by  $Co^{60}$  source in order to reproduce at least to some extent cosmic background. Comparison of the data with and without  $Co^{60}$  source showed no difference in trailing pixel distribution, which is consistent with our understanding of the emission mechanisms. Data were taken at several different temperatures, the results are shown on Fig. 7. Solid lines on the plot are the results of the multiexponential fits to the data, experimental points are also shown on the plot. We did not put the results on the same plots with flight data because we have yet to get more accurate



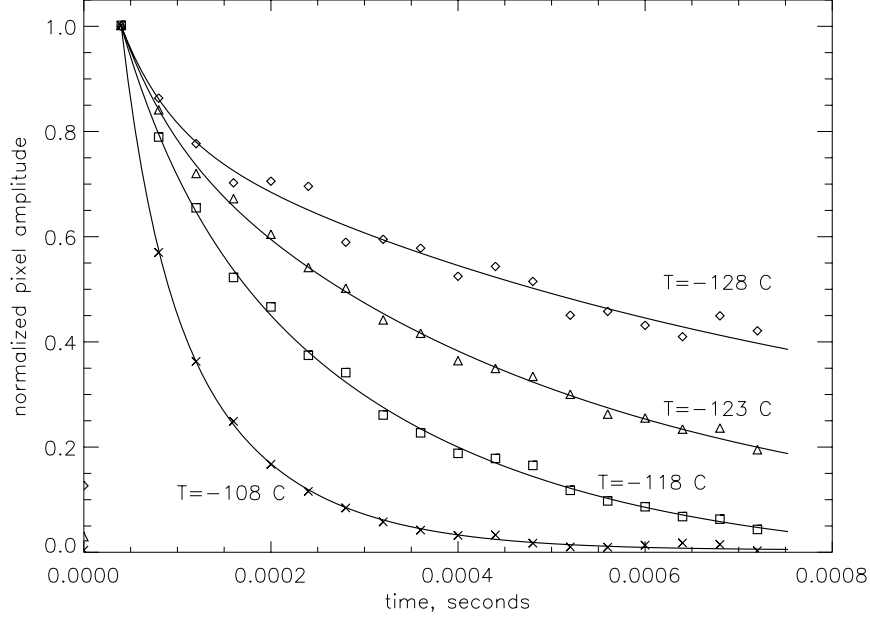


**Figure 7.** Trailing pixel amplitudes behind  $Mn K_{\alpha}$  events at different temperatures.

calibration of the temperature in the ground setup relative to the flight instrument. Qualitatively temperature dependence of the trailing pixel curves seem to agree well with the flight results.

#### 4.2. “Squeegee” technique

There is a population of traps in the buried channel with emission time constants exceeding frame integration time. If such traps are filled in the beginning of each frame, their impact on the X-ray events could be significantly diminished. Significant fraction of these traps will stay filled until the end of integration period and signal charge packets would not lose electrons to them. In order to verify this a peculiar clocking scheme which we called “squeegee” technique was implemented. Chandra CCDs do not have any means to inject charge into the imaging array, so we used particle-generated background to collect charge into the few rows at the boundary of the array. A  $Co^{60}$  source was placed near the CCD during the testing to produce charge in the device.

Both sections of the device have 1026 rows. During the fast transfer from image to frame store section the number of transfers was made smaller than the number of rows in the image section. Only  $1026 - N_{tr}$  vertical transfers were made, where  $N_{tr}$  is a small arbitrary number. This means that  $N_{tr}$  rows were left at the bottom of the image section not transferred out. Then, during the slow readout cycle from frame store into serial register the image section was clocked backwards and the bottom  $N_{tr}$  rows were shifted to the top of the array. In the next frame the whole sequence is repeated. Thus, the  $N_{tr}$  rows are never read out and after several cycles they accumulate enough charge from the particle background to be able to fill the traps in the imaging array in every passage from the bottom to the top. In our experiments we varied the number of accumulating rows  $N_{tr}$ , and there seem to be a minimum below which they do not perform their function of filling the traps.

As usual,  $Fe^{55}$  radioactive source was used to measure the CTI of the device. Results are very encouraging. On Fig. 8 is shown a plot of the full width half maximum (FWHM) of the  $Mn K$  line as a function of row number for the data taken with and without “squeegee” clocking. The number of accumulating rows in this case was 48. At the top of the array the reduction of the FWHM is more than by a factor of 2, which is huge improvement.

This technique is very efficient in improving the energy resolution of the device, while improvement in CTI is very modest. “Squeegee” technique suppresses the traps with time constant longer than frame time and we showed before that such traps are responsible for about 20% of the charge loss. Because of that it does not have strong effect on the CTI. On the other hand, the same traps are mostly responsible for the loss of energy resolution because the charge loss to these traps changes depending on the distance to the previous event. This could be a promising technique

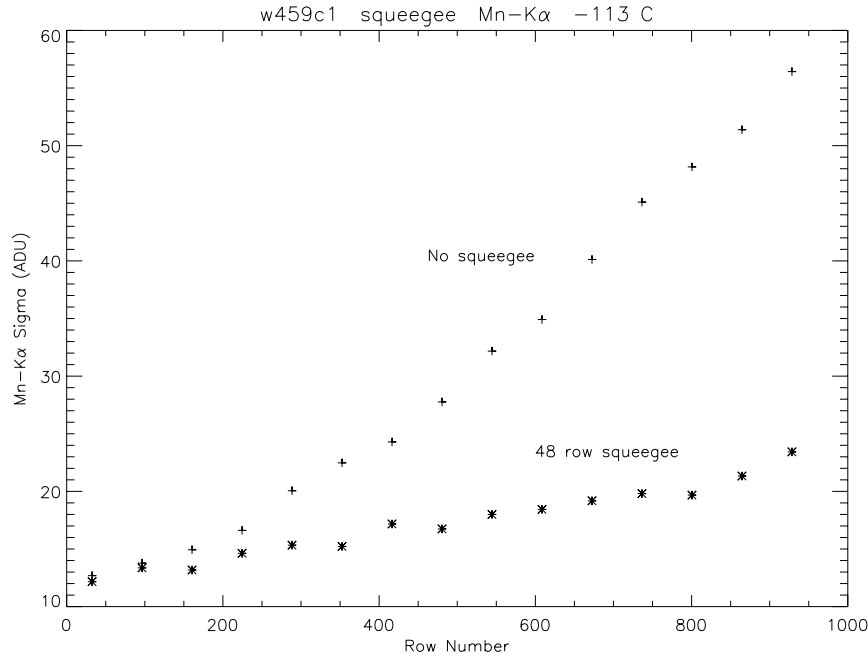


**Figure 8.** Full width half maximum of the  $Mn K_{\alpha}$  peak as a function of row number for the data with “squeegee” and regular clocking.

which may noticeably mitigate radiation damage effects in the flight devices. At the moment we are planning to test this technique for the flight focal plane.

## 5. CONCLUSION

We have analysed radiation damage in the frontside illuminated CCDs comprising Chandra focal plane. We have developed new techniques for radiation damage characterization and trap parameters measurement. These techniques allowed us to measure trap emission time constants and determine that there are at least three different trap energy levels in the flight devices. The damage characteristics are consistent with the type of damage we observed on the ground after irradiating similar chip with low energy (102 keV) protons. We were able to determine that the frame store sections of the flight devices remained intact which is also consistent with the low energy proton hypothesis. We have developed a peculiar clocking scheme (“squeegee” mode) which in ground experiments seem to significantly improve device performance by filling traps with long time constants in the beginning of each frame.

## 6. ACKNOWLEDGEMENTS

This work was funded by NASA under the contract NAS-37716.

## REFERENCES

1. S. L. O'Dell, M. W. Bautz, W. C. Blackwell, Y. M. Butt, R. A. Cameron, R. F. Elsner, M. S. Gussenhoven, J. J. Kolodziejczak, J. I. Minow, D. A. Swartz, A.F. Tennant, S. N. Virani, and K. Warren, "Radiation environment of the Chandra X-ray Observatory" SPIE meeting, San Diego, 2000, submitted
2. K.Gendreau, G.Prigozhin, R.Huang, M.Bautz,"A technique to measure trap characteristics in CCD's using X-rays", IEEE Transactions on Electron Devices, v. 42, No. 11, pp. 1912-1917, 1995
3. K.Gendreau, M.Bautz, G.Ricker, "Proton damage in X-ray CCDs for space applications: Ground evaluation techniques and effects on flighe performance", Nuclear Instruments and Methods in Physics Research, A, v.335, pp.318-327, 1993
4. A. Holland,"The effect of bulk traps in proton irradiated EEV CCDs", Nuclear Instruments and Methods in Physics Research, A, v.326, pp. 335-343, 1993

5. T.Hardy, R.Murowinsky, M.Deen," Charge transfer efficiency in proton damaged CCD's", IEEE Transactions on Nuclear Science, vol. 45, No.2, Apr. 1998, pp.154-163
6. C. Dale, P.Marshall, B.Cummings, L.Shamey, A.Holland, "Displacement damage effects in mixed particle environments for shielded spacecraft CCDs", IEEE Transactions on Nuclear Science, vol. 40, No. 6, pp. 1628-1636, Dec. 1993
7. J.Janesick, G.Soli, T.Elliot, S.Collins," The effect of proton damage on charge-coupled devices", Proc. SPIE, vol. 1447, pp.87-108, 1991